Original Research

Journal of Advanced Veterinary Research
(2024) Volume 14, Issue 5, 807-812

Effect of silica nanoparticles on kidney of albino rats with the potential ameliorative efficacy of liposomal curcumin

Hala Youssef[1*], Yasmine A. Mansour[1], Ebtihal M.M. EL-Leithy[1,2], Mona K. Galal[3], Maha M. Rashad[3], Emad Tolba[4], Khaled S. Abou-El-Sherbini[5], Mamdouh A. El-Shammaa[1]

[1]*Cytology and Histology Department, Faculty of Veterinary Medicine, Cairo University, Giza 12211, Egypt.*
[2]*Anatomy and Histology Department, Faculty of Veterinary Medicine, Egyptian Chinese University, Cairo,11771, Egypt.*
[3]*Biochemistry and Chemistry of Nutrition Department, Faculty of Veterinary Medicine, Cairo University, Giza12211, Egypt.*
[4]*Polymers and Pigments Department, National Research Centre, 33 El Bohouth St, Dokki, Giza, 12311 Egypt.*
[5]*Department of Inorganic Chemistry, National Research Centre, 33 El Bohouth St. (former Eltahrir st.), Dokki, Giza, P.O.12622, Egypt.*

ARTICLE INFO

Recieved: 02 January 2024

Accepted: 09 February 2024

***Correspondence:**

Corresponding author: Hala Youssef
E-mail address: halayoussefmontash@gmail.com

Keywords:

Silica nanoparticles (SiO_2-NPs)
Liposomal curcumin (LP-Cur)
Apoptosis, Nephrotoxicity
Oxidative stress

ABSTRACT

Silica nanoparticles (SiO_2-NPs) are widely used commercially in various biomedical and industrial applications. However, their potential toxicity on human and animal health has attracted particular attention. Liposomal curcumin (LP-Cur) has effective antioxidant and anti-inflammatory defense mechanism. So, this study was achieved to assess the potential ameliorative effect of (LP-Cur) on (SiO_2-NPs) induced nephrotoxicity in rats. Twenty four adult male albino rats weighing 170.0±20.0 g, were divided into four groups: (Gp I) negative control group (received single intraperitoneal injection of 0.9% saline, standard diet and distilled water), (Gp II) SiO_2-NPs exposed group (received 200 mg/kg body weight intraperitoneally), (Gp III) SiO_2-NPs and LP-Cur co-treated group (received 200 mg/kg body weight SiO_2-NPs intraperitoneally + 80 mg/kg body weight LP-Cur orally), and (Gp IV) LP-Cur treated group (received 80 mg/kg body weight orally) for 30 days. At the end of experiment, the rats were anaesthetized with diethyl ether in internal volume of chamber. Blood and kidney samples were collected from all rats for biochemical, histopathological and immunohistochemical analyses. SiO_2-NPs significantly increased blood urea nitrogen (BUN), serum creatinine levels and malondialdehyde. Whereas they substantially reduced the glutathione levels. SiO_2-NPs also caused dilatation, congestion ofmost glomeruli in addition to, some atrophied ones. Also, most renal tubules showed degenerative changes and marked interstitial hemorrhage. A significant increase in the immunoreactions of caspase-3 of SiO_2-NPs exposed rats. Conversely, the administration of LP-Cur ameliorated the detrimental toxic effects caused by SiO_2-NPs. In conclusion, antiapoptotic and antioxidant actions of LP-Cur ameliorate the nephrotoxic effect induced by SiO_2-NPs.

Introduction

Nanotechnology has gained more importance over the past few decades and used in wide varieties of fields as agriculture, pharmaceutical industries (Hozayen *et al*., 2019), biomedical application as tumor diagnosis and therapy as drug carriers in targeted drug delivery (TDD) or in biodegradable implants as on laser tissue soldering (LTS) (Liang *et al*., 2018) which considered an alternative method of treatment for injuries of hollow organs as blood vessels which help in faster procedure time, immediate water tightness, reduced recovery time, faster wound healing in comparison to classical micro suturing (Puca *et al*., 2006; Bogni *et al*., 2012). On the other hand, nanoparticles are considered as foreign materials and so may cause adverse effects when they come in contact with the body tissues and cells. As many nanoparticles cannot be effectively eliminated, they accumulate in the body (Wang *et al*., 2004) and affect the biological behavior of tissue and organs (Schrand *et al*., 2010).

According to the Consumer Products Inventory (CPI), SiO_2-NPs were found in over 100 commercial products including foods, toothpastes, cosmetics, paints, electrical gadgets, and even medications and vitamins (Vance *et al*., 2015). Because of its numerous applications, SiO_2-NPs have become the second most important engineering nanomaterial in terms of annual output (WHO, 2017). The human body can be intentionally or unintentionally exposed to SiO_2-NPs by inhalation, oral intake, transdermal penetration, and parenteral injection (Yazdimamaghani *et al*., 2018). SiO_2-NPs have the potential to spread almost all organs and, either directly or indirectly, result in tissue damage and inflammation (Guo *et al*., 2013). As previously reported, SiO_2-NPs induce hazardous effects as oxidative stress which plays an important role in increasing ROS, lipid peroxidation (LPO) and depletion of glutathione (GSH) which in turn leading to cell membrane damage, DNA damage, mitochondrial dysfunction, cell cycle arrest, necrosis, and apoptosis (Aillon *et al*., 2009; Sun *et al*., 2011) leading to marked histopathological alterations (Guo *et al*., 2013).

The kidney is particularly susceptible to toxins due to its extensive vascularization for blood filtration and removal of toxic compounds and their metabolites from the body (Gazia and El-Magd, 2019; Florek *et al*., 2023). Kidney is known as one of the most vulnerable organs after exposure to nanoparticles (Kim *et al*., 2008). SiO_2-NPs can be carried into the bloodstream and deposit in target organs where the nanoparticles may have harmful effects after translocating across biological barriers (Fruijtier- Pölloth, 2012).

Curcumin (1,7-bis(4-hydroxy-3-methoxyphenyl)-1,6-heptadiene-3,5-dione) is a naturally occurring polyphenolic compound which derived from the rhizome of the herb Curcuma longa (Rai *et al*., 2010; Ghalandarlaki *et al*., 2014; Hewlings and Kalman, 2017). Curcumin exhibits anti-inflammatory, antioxidant (Jurenka, 2009), anti-microbial and anti-carcinogenic actions (Manconi *et al*., 2007; Nalli *et al*., 2017). It can improve cell viability in various disorders by reducing the cell apoptosis and necrosis (Shehzad *et al*., 2017). The antioxidant potential of curcumin is derived from its ability to scavenge the reactive oxygen species (ROS) (Jurenka, 2009; Yu *et al*., 2011). Curcumin also inhibited apoptosis induction in renal tissue by inhibiting transforming growth factor-beta (TGF-β) and caspase-3 (Awad and El-Sharif, 2011).

As the oral bioavailability and plasma solubility of curcumin are limited, the liposomal formulations were developed (Storka *et al*., 2013) which can enhance its systemic bioavailability and tissue distribution (Gera *et al*., 2017). The utilization of liposomesenhances the water solubility of curcumin, resulting in a notable 8- to 20-fold rise in systemic exposure when compared to the conventional curcumin suspension formulation (Hamano *et al*., 2019). Liposomes were first developed from self-forming

ISSN: 2090-6277/2090-6269/

encapsulated lipid bilayers (Bangham, 1993). Liposomes are made up of a hydrophilic inner aqueous chamber and a hydrophobic lipid bilayer; high percentages of lipophilic medicines can spread in the lipid bilayers (Signorell *et al*., 2018). Liposomes have generated a lot of attention in the field of drug delivery due to its ability to load drugs, biodegradability, biocompatibility, and ability to prevent immunological reactions (Joshi *et al*., 2019). Curcumin's water-solubility and stability were significantly improved after being enclosed in liposomes, according to Wei *et al*. (2020).

Materials and methods

Chemicals

The Tetraethyl orthosilicate (TEOS) was acquired from Sigma-Aldrich Chemical Co (St. Louis, USA). Liposomal curcumin was purchased from Healthy Drops.

SiO_2-NPs synthesis by Sol-Gel method

The SiO_2-NPs were prepared by hydrolyzing TEOS (silica precursor) in a mixture of water, methanol, and ammonia (as a catalyst). In a typical synthesis approach, 10 ml of TEOS solution were added to 20 ml methanol and 80 ml deionized water. The reaction container was kept under vigorous stirring at 1000 rpm for 10 min and then ultrasonicated for 10 min for homogeneity. Then, ammonia solution (28-30%, Sigma Aldrich) was added drop wise to the mixture to the methanolic aqueous solution of TEOS over 10 min period. The reaction pH was adjusted at 11. The clear reaction mixture slowly turned turbid due to SiO_2-NPs formation. The reaction was kept under stirring for 4 h at room temperature. The obtained white gel was collected via centrifugation and washed twice with methanol solution (50%). Finally, the wet SiO_2-NPs were air-dried at 80°C for 48 h. and crushed to obtain nano-powder using an agate mortar, followed by sieving to avoid agglomeration.

Morphological observation

The examination of the particle morphology and size of the nanoparticles that were generated was conducted using JEOL 1010 transmission electron microscopy at Faculty of Agriculture, Cairo University, Egypt.

Experimental protocol and animal grouping

Experimental animals and ethical approval

Twenty four mature male albino rats of the same weight (170.0±20.0 g) were bought from the animal house of VACSERA, Egypt. Before the experiment, the animals had a two-week adaptation period. They were kept in polypropylene cages with a 12/12 h light/dark cycle, a room temperature of 22.0±2.0°C, and a relative humidity of 50±10%. They were given unlimited access to food and water. The Institutional Animal Care and Use Committee (IACUC) of Cairo University's Faculty of Veterinary Medicine approved the experimental protocols (Protocol no: Vet CU 03162023645). In accordance with National Institutes of Health (NIH) guidelines, rats were handled humanely.

Experimental design

Rats were randomly divided into four groups (n.= 6) following the time of acclimatization. Gp I (negative control): Rats received daily 0.9% saline intraperitoneally for 30 days (Mahmoud *et al*., 2019). Gp II (SiO_2-NPs administrated group): Rats treated with SiO_2-NPs intraperitoneally at a dose of 200 mg/kg (Mahmoud *et al*., 2019). GpIII: SiO_2-NPs (200 mg/kg/d) and LP-Cur orally at (80 mg/kg/d) were co-administered to the rats. Gp IV: LP-Cur (80 mg/kg/d) was administered to rats. That was for 30 days (Alhusaini *et al*., 2018).

Sample collection and preparation

Following a treatment period of 30 days, the rats were anaesthetized with diethyl ether. After that, blood samples were collected from the ocular plexus and placed in sterile glass tubes, where they would coagulate for 20 minutes at room temperature. The blood samples were centrifuged at 3000 rpm for 10 minutes to separate the serum and stored at -20°C for determination of kidney function tests. Then, after cervical dislocation, each kidney was taken immediately. A portion of the samples were kept at -80°C to measure the parameters of oxidative stress. Other samples were placed in 10% neutral buffered formalin (NBF) for 24 to 48 hours for further histopathological and immunohistochemical investigations.

Biochemical analyses

Determination of kidney biomarkers (kidney function tests)

Blood urea nitrogen (BUN) was estimated using urease colorimetric method and serum level of creatinine was measured by Kinetic jaffé reaction. The procedures were conducted according to reagent kits following the given instructions (spectrum diagnostics. Egyptian Company for Biotechnology).

Renal oxidative stress biomarkers

Renal tissue was homogenized in an ice-cold 0.1-M phosphate-buffered saline (pH 7.4) using tissue homogenizer. The crude tissue homogenate was centrifuged at 15,000 rpm for 15 min at 4°C and used to determine malondialdehyde (MDA) according to Ohkawa *et al*. (1979) and reduce glutathione (GSH) according to Ellman (1959).

Histopathology and immunohistochemistry

Light microscopy

The kidney specimens were subjected to dehydration using a series of ascending ethanol dilutions. After that, the samples underwent two successive rinses in xylene, followed by embedding in paraffin wax and subsequent sectioning to paraffin sections of 3-4 µm. The de-waxed serial slices underwent staining with hematoxylin and eosin (H&E) for histological examination (Bancroft and Gamble, 2008).

Immunohistochemistry of Caspase-3

4-µm renal sections were mounted on positive charged glass slides for detection of apoptosis by Avidin-biotin peroxidase complex (Hsu *et al*., 1981). The antibodies used were anti caspase-3 antibody and active form formed in rabbit (AB3623, EMD Millipore) (active/cleaved) (Novus Biologicals "100-56113"). Sections were incubated with previously stated antibodies and then the appropriate reagent for the Avidin-Biotin-Peroxidase Complex procedure (Vecta stain ABC-HRP kit, Vector Laboratories) was applied. Each marker expression was labelled using peroxidase and colored with diaminobenzidine substrate (DAB, Sigma) for antigen-antibody complex revealing.

Assessment of the immunohistochemical sections

Caspase-3 stained renal sections were assessed using Leica Quin 500 analyzer computer system (Leica Microsystems, Switzerland) in the Faculty of Dentistry, Cairo University. The image analyzer underwent an automatic calibration process to convert pixels into micrometer units. The immune reactivity of Caspase-3 was quantified as a percentage of the

total area within a standardized measuring frame. This measurement was performed in 10 fields from distinct slides for each experimental group, utilizing a magnification of (400X) under light microscopy. All regions exhibiting brown immune staining positive for caspase-3 were chosen for evaluation, regardless of the intensity of the immune staining. The mean value and standard error of the mean (SEM) were calculated for each specimen and subjected to statistical analysis.

Statistical analysis

All data was initially inspected for normality, after that they were subjected to a one-way analysis of variance (ANOVA) to determine the mean significance between groups. The results were expressed as the mean ± standard error of the mean (SEM) which was after that verified by a least significant difference (LSD) post hoc test. A p-value ≤ 0.05 was statistically significant. All data were analyzed by SPSS version 17.0 software (IBM, USA).

Results

Characterization of Silica nano particles

Transmission electron microscopy (TEM) of the prepared SiO_2-NPs was displayed spherical particles with an average size 108.80±9.6 nm (Fig. 1).

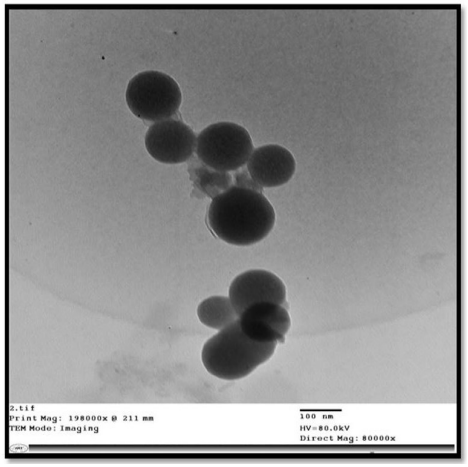

Fig. 1. Spherical shaped SiO_2- NPs with an average size 108.80± 9.6 nm.

Biochemical investigations

Effect of SiO_2-NPs and LP-Cur on kidney function

BUN and creatinine levels were used for evaluation of renal damage. Fig. 2 reveals that SiO_2-NPs induced asignificant (p≤ 0.05) increase in BUN level from 6.3 to 11.8 mg/dL and serum creatinine level from 0.6 to 0.75mg/dL when compared with the control group. In comparison with SiO_2-NPs group, co-treatment with LP-Cur significantly (p≤0.05) reduced BUN. Similarly, co-treatment with LP-Cur significantly (p≤ 0.05) reduced serum creatinine.

Effect of SiO_2-NPs and LP-Cur on oxidative stress biomarkers

Renal content of GSH

Compared with a control group, renal GSH content was significantly (p≤ 0.05) reduced from 152.033 to 68.12 in rats treated with SiO_2-NPs. Co-treatment with LP-Cur significantly (p≤ 0.05) elevated GSH to 95.88 in comparison with SiO_2-NPs treated group as shown in Fig. 3.

MDA content in renal tissue

According to the data obtained in (Fig. 3), treatment with SiO_2-NPs significantly (p≤ 0.05) elevated renal MDA content from 329.2 to 764.8 μMg^{-1} tissue when compared with the control group. On the other hand, LP-Cur treatment successed to induce a significant (p≤ 0.05) reduction in renal MDA content to 472 μMg^{-1} tissue in comparison with SiO_2-NPs-group.

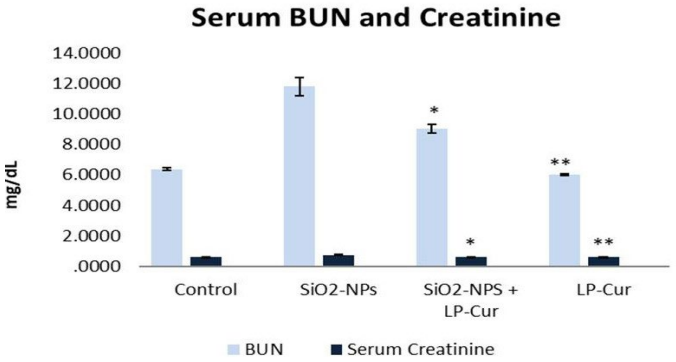

Fig. 2. Effects of LP-Cur and SiO_2-NPs on serum BUN and creatinine (mg/dL) in male rat. Data are represented as mean ± SEM. *indicates significant difference from the corresponding control negative group at p≤0.05. ** indicates significant difference from the SiO_2-NPs treated group at p≤ 0.05.

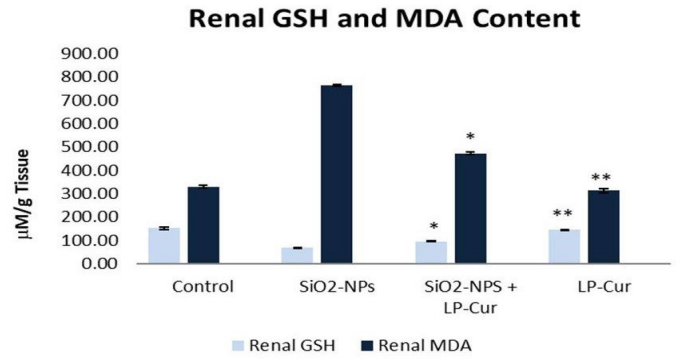

Fig. 3. effects of LP-Cur and SiO_2-NPs on renal GSH and MDA (µM g-1 tissue) in male rat. Data are represented as mean ± SEM. *indicates significant difference from the corresponding control negative group at p≤ 0.05. ** indicates significant difference from the SiO_2-NPs treated group at p≤ 0.05.

Histopathological examination

Light-microscopy findings

The light microscopic examination of H&E stained renal tissues obtained from the control rats (GP I) showed a normal histological architecture of the renal cortex that consisted of renal corpuscle, proximal and distal convoluted tubules. The renal corpuscle consisted of a normal glomerular capillary tuft with patent urinary space enveloped by Bowman's capsule. The proximal convoluted tubules (PCT) were lined by truncated pyramidal cells with narrow lumina and the distal convoluted tubules (DCT) were lined by cuboidal cells with wide lumina (Fig. 4a).

By contrast, renal tissue sections obtained from rats exposed to SiO_2-NPs (GpII) revealed various histopathological alterations in the renal cortex as compared to the control group. Most renal corpuscles exhibited marked dilatation and congestion of the glomerular capillaries with narrow capsular space. Whereas others displayed degeneration and shrinkage of the glomeruli with an expanded capsular space. Most PCT and DCT exhibited marked degenerative changes represented by loss of normal histoarchitecture with pyknosis of the nuclei of their lining cells that frequently sloughed into the lumen (Fig. 4b). Furthermore, few cytoplasmic contents are lost into the lumen of some DCT tubules (Fig. 4c). Additionally, some DCT revealed pronounced loss of cytoplasmic acidophilia of

their lining epithelial cell accompanied by pyknosis of their nuclei (Fig. 4b) and others exhibited marked lysis of the lining cells' cytoplasm with pyknosis of their nuclei which occasionally appeared elongated. Some tubular cells of PCT partially lost their cytoplasmic acidophilia and others appeared with elongated pyknotic nuclei (Fig. 4d). Vascular congestion and inflammatory cell infiltration (Fig. 4c) in addition to, marked interstitial hemorrhage were noticed in the cortex (Fig. 4d).

On the other hand, the SiO_2-NPsexposed rats co-treated with LP-Cur (Gp III) exhibited remarkable improvement in the histological structure of the kidney. The renal cortex appeared apparently normal with less tubular degeneration (Fig. 4e).

Conversely, renal sections obtained from rats exposed to LP-Cur (Gp IV) showed a normal histoarchitecture similar to that observed in the control group (Fig. 4f).

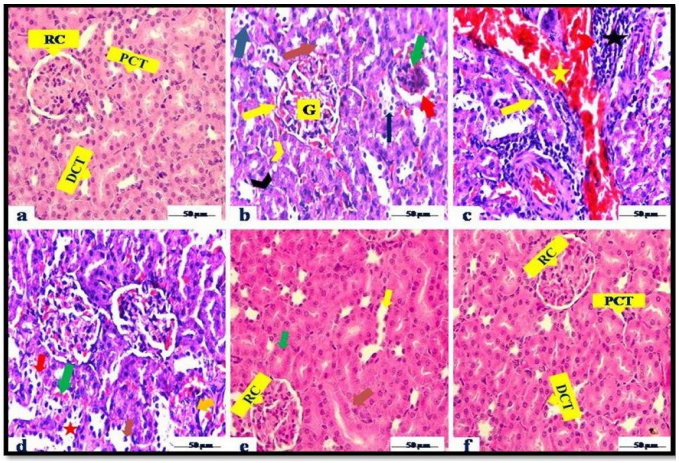

Fig. 4. A photomicrograph of H&E stained sections of albino rats' renal cortex (a) Control group (GP I)showing normal histological structure of the renal corpuscle (RC), proximal convoluted tubule (PCT) and distal convoluted tubule (DCT) (x400). (b:d) SiO_2-NPs exposed group (GP II) showing (b) Dilated and congested glomerular capillaries (G) with narrow capsular space (yellow arrow), shrunken and degenerated glomerulus (green arrow) with wide urinary space (red arrow), degeneration of most PCT (black chevron) and DCT (yellow chevron) with loss of their normal histoarchitecture, complete loss of cytoplasmic acidophilia of the lining epithelial cells of some DCT (black arrow) in addition to, some tubular cells of PCT partially lost their cytoplasmic acidophilia (brown arrow). Notice: sloughed nucleus of some tubular cells in the lumen (blue arrow) (x400). (c) Vascular congestion (yellow star) and inflammatory cell infiltration (black star). Notice: cytoplasmic strands in the lumen of DCT (yellow arrow) (x400). (d) Showing some degenerated DCT with lyses of their lining cells (red star), pyknosis of their nuclei (brown arrow) which occasionally appeared elongated (red arrow). Elongated pyknotic nuclei of some tubular cells of PCT (orange arrow). Notice: Interstitial haemorrhage (green arrow) (x400). (e) SiO_2-NPs exposed rats co-treated with LP-Cur (GP III) revealing restoration of histological structure of the renal corpuscle with nearly normal renal corpuscle (RC), PCT (green arrow) and DCT (brown arrow) whereas, some tubules still showed degeneration (yellow arrow) (x400). (f) LP-Cur administered group (GP IV) showing normal renal corpuscle (RC), proximal convoluted tubule (PCT) and distal convoluted tubule (DCT) (x400).

Moreover, the renal medulla sections obtained from the control rats (Gp I) exhibited a typical histoarchitecture of the collecting tubules that were lined with simple cuboidal cells, loop of Henel's, and interstitial blood capillaries (Fig. 5a). While, the renal tissue of SiO_2-NPs rats exposed rats (Gp II) exhibited various histolopathological alterations in the renal medulla. Most collecting tubules revealed pronounced degeneration with shedding of cytoplasmic contents as well as some nuclei in their tubular lumina whereas, others revealed loss of their lining epithelial cells' cytoplasmic acidophilia with pyknosis of most nuclei. Other degenerated collecting tubules lost their normal cellular details with pyknotic nuclei which occasionally appeared flattened. Furthermore, marked interstitial hemorrhage was observed between the degenerated tubules (Fig. 5b).

On the other hand, markedrecovery of the renal medulla with few degenerated collecting tubules as well as slight interstitial hemorrhage were observed in the SiO_2-NPs exposed group co-treated with LP-Cur (Gp III) (Fig. 5c). On country, renal sections obtained from rats treated with LP-Cur (Gp IV) revealed a normal histological structure similar to that observed in the control group (Fig. 5d).

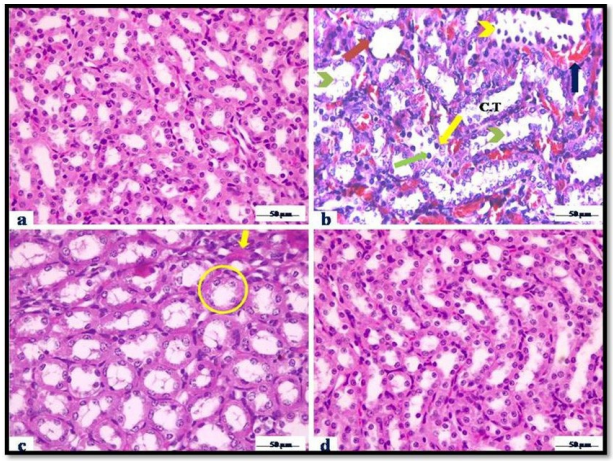

Fig. 5. A photomicrograph of H&E stained sections of albino rats' renal medulla (a) Control group (GP I) revealing intact histological structure of collecting tubules(x400). (b) SiO_2-NPs exposed group (GPII) showed most degenerated collecting tubules (C.T) appeared with cytoplasmic contents (green chevron) and or sloughed nuclei (yellow chevron) into their lumina and others revealed loss of cytoplasmic acidophilia of their lining cells (green arrow) with pyknosis of most nuclei (yellow arrow) in addition to, some degenerated collecting tubules lost their normal cellular details with flattened pyknotic nuclei (brown arrow). Notice marked interstitial haemorrhage (black arrow) (x400). (c) SiO_2-NPs exposed rats co-treated with LP-Cur (GP III) revealing restoration of histological structure of renal medulla with less degenerated tubules (yellow circle) and slight interstitial hemorrhage (yellow arrow) (x400). (d) LP-Cur administered group (GP IV) showing normal histoarchitecture of the collecting tubules (x400).

Immunohistochemical observations for caspase-3

Renal tissues obtained from the control rats (Gp I) exhibited negligible caspase-3 immunoreaction (Fig. 6a). Whereas, the SiO_2-NPsexposed group displayed intense caspase-3 positive immunoreactions (Fig. 6b). In contrast, the renal sections obtainedfrom rats that co-administrated SiO_2-NPs and LP-Cur (Gp III) showed a weak immunoreaction for caspase-3(Fig. 6c). Inaddition, the LP-Cur exposed group (GpI V) showed negligible immunoreactivity to caspase-3 reaction like the control group (Fig. 6d).

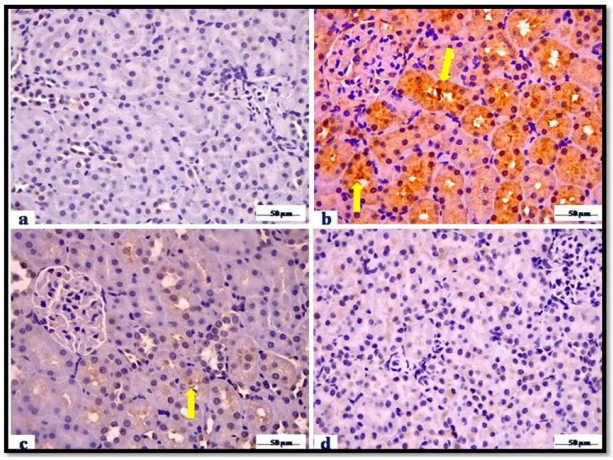

Fig. 6. A photomicrograph of caspase-3 immunoreaction in the renal cortex sections (x400). (a) Negligible caspase-3 immunoreaction in the renal tissue obtained from the control group (GP I). (b) Intense positive immunoreactions (yellow arrows) in the tubular epithelium of SiO_2-NPs exposed group (GP II). (c) Mild caspase-3 expression (yellow arrows) in the SiO_2-NPs exposed rats treated with LP-Cur (GP III) (d) Negligible caspase-3 immunoreaction in the LP-Cur treated group (GP IV).

Immunohistochemical findings

Data analysis revealed a significant ($p \leq 0.05$) increase in the area percentage covered by caspase-3 positive immunoreactive cells within the kidney of SiO_2-NPs exposed group by 54.740 fold as compared to control group. On the other hand, Co-treatment with LP-Cur significantly ($p \leq 0.05$) decreases caspase-3 area percentage mediated by SiO_2-NPs by 16.804 fold. As shown in Table 1.

Table 1. The ameliorative effect of LP-Cur supplementation on the area occupied by caspase-3 positive immunoreactive cells in renal sections of SiO_2-NPs exposed rats.

Groups	Area occupied by caspase-3 positive immunoreactive cells (%)
Gp (I)	1.181±0. 128^{c}
Gp (II)	54.740±2.465^{a}
Gp (III)	16.804±0.657^{b}
Gp (IV)	1.135±0.127^{c}

Values are presented as Mean±SEM, the different superscripts (^{a,b,c}) within the same column reflect significant differences at P≤ 0.05.

Discussion

With the wide spread use of SiO_2-NPs in agriculture, cosmetics, commodity, and medicine, their toxicity to the animal body is a concern (Kim *et al*., 2014). The kidneys are the main metabolic organs of the body and are considered the main route of nanomaterial excretion (Almeida *et al*., 2011). The kidneys, liver, lungs, and spleen considered as the target organs for SiO_2-NPs (Lee *et al*., 2014; Liang *et al*., 2018). Those authors also, reported that SiO_2-NPs were found to persist longer in kidneys and liver than any other organ. The mechanism of renal toxicity caused by SiO_2-NPs is complex and remains unclear. In the present study, we evaluated the sub acute toxicity of SiO_2-NPs exposure and the protective effect and the possible mechanism of LP-Cur on renal impairment caused by SiO_2-NPs exposure in rats.

The analysis of renal biomarkers (BUN and creatinine) and oxidative stress indicators (GSH and MDA) was used to monitor the protective impact of LP-Cur against SiO_2-NPs produced renal oxidative damage. BUN is thought to be a main strong renal biomarker that increases in the event of any kind of renal damage. Another renal biomarker that increases in response to reduced glomerular filtration rate is serum creatinine, so we measured the serum BUN and creatinine which are considered the two classical clinical markers of renal dysfunction (Ahmed *et al*., 2022). The levels of BUN and creatinine were markedly increased in the SiO_2-NPs intoxicated group compared to control one suggesting a significant renal damage induced by SiO_2-NPs. Since BUN and creatinine are produced during purine metabolism, their elevated serum levels could indicate filtration rate alterations and be linked to kidney injury (El Gamal *et al*., 2014). These outcomes are in line with those of other researchers (Hassankhani *et al*., 2015; Badawy *et al*., 2023) which indicating the nephrotoxicity of SiO_2-NPs.The decreased concentrations of kidney biomarkers in LP-Cur treated rats indicate its defensive effects on kidneys. LP-Cur increases the secretory function of kidney leading to remove the toxic substance from the blood (El-Desoky *et al*., 2022) thus helps to protect the kidney tissues from SiO_2-NPs -induced nephrotoxicity. The nephro-protective influence of LP-Cur was reported by several research (El-Desoky *et al*., 2022; Machado *et al*., 2022).

Oxidative stress is one of the potential mechanisms of renal toxicity induced by SiO_2-NPs. Under normal condition, there is a balance between ROS production and antioxidant elimination. When this balance is broken, several cellular components could be injured (Birben *et al*., 2012). In order to clarify the antioxidant effect of LP-Cur on SiO_2-NPs induced nephrotoxicity in rats, the contents of malondialdehyde (MDA) and glutathione (GSH) in the tissue homogenates were measured as the indicators for evaluating the levels of oxidative stress in kidney. Compared to control, the content of MDA, a classic indicator of oxidative stress, showed a significant elevation, while the level of GSH (an intracellular free radical scavenger nonenzymatic antioxidant) was markedly decreased in the SiO_2-NPs intoxicated group, suggesting SiO_2-NPs -induced elevation of oxidative stress and decrease of antioxidant capacity in the kidney. The present data are in line with Badawy *et al*. (2023) who suggested that SiO_2-NPs increased ROS production and reduced the antioxidant defense for renal tissue. Recent studies have shown that SiO_2-NPs increase the production of ROS, which deplete endogenous antioxidants and damages biological macromolecules such as nucleic acids, lipids, and proteins (Sun *et al*. 2021; Almanaa *et al*., 2022; Badawy *et al*., 2023). ROS over production is considered an essential mechanism for SiO_2-NPs induced cell damage (Murugadoss *et al*., 2017) owing to the release of active oxides in cells causing oxidative damage (Fritsch-Decker *et al*., 2018). As expected, LP-Cur treatment significantly reversed these alterations induced by SiO_2-NPs suggesting that the antioxidative property of curcumin. The powerful antioxidant effects of LP-Cur were reported by several research paper (Liu *et al*., 2022; Noor *et al*., 2022; Salimi *et al*., 2022). The antioxidant activity of curcumin is mediated by the electron donating groups of curcumin especially the phenolic hydroxyl group (Zheng *et al*., 2017). In addition, curcumin elevates the activity and expression level of antioxidant enzymes (Wu *et al*., 2020). Toxicology studies have suggested that SiO_2 NPs can induce adverse effects in the liver, kidney and brain (Nemmar *et al*., 2016; Chan *et al*., 2017; Almansour *et al*., 2018)

In the current study, the renal tissue of SiO_2-NPs -exposed rats (GP I) displayed multiple histopathological alterations as compared with control rats such as dilatation and congestion of glomerular capillaries, that agrees with the result of Azouz and Korany (2021) and Abdelhalim and Jarrar (2011) in the renal cortex of Wistar rats intraperitoneally administered 10 nm to 20 nm of gold nanoparticles (GNPs) for 7 days. This dilatation might be attributed to the direct impact of nanoparticles on the lining cells of the blood vessels, which might result in the release of nitric oxide, the endothelial relaxation factor and consequently vasodilatation (Xia *et al*., 2006). Furthermore, some renal corpuscles showed shrinkage and degeneration as reported with Mahmoud *et al*. (2019) and Azouz and Korany (2021). Histological changes of renal corpuscles might reflect impaired renal function (Mohamed and Salah, 2010).

Most renal tubules (PCT and DCT) displayed marked degenerative changes in the form of loss of normal histoarchitecture with cytoplasmic and nuclear changes mainly pyknosis. The same findings was reported by Ahmed *et al*. (2021) in renal tissue of orally administered 3% PS-NPs (polystyrene nanoparticles) (3 mg/kg body weight/day) for 35 days. Moreover, inflammatory cell infiltration was observed in the renal cortex that correlated with Mahmoud *et al*. (2019); Azouz and Korany (2021) and Mehdi and Al-Husseini (2021)'s findings. Johar *et al*. (2004) reported that gold nanoparticles (GNPs) could interact with the enzymes and proteins of the interstitial tissue of kidney inhibiting the antioxidant defense mechanism and ROS generation, which may trigger an inflammatory response.

In the current work, the collecting tubules in the renal medulla displayed histopathological changes that manifested as degeneration accompanied by cytoplasmic strand shedding and some sloughed nuclei in their tubular lumina. Others reported that their cells' cytoplasmic acidophilia had been lost, along with pyknosis of the majority of their nuclei, which occasionally seemed flattened. This was in accordance with Ahmed *et al*. (2021)'s findings.

Additionally, marked interstitial hemorrhage was observed in the renal cortex and medulla between the tubules which might be attributed to abnormal coagulation system activation following administration of SiO_2-NPs. This could lead to a decrease in coagulation factors and an increase in vascular permeability (Nabeshi *et al*., 2012).

On the other hand, this study showed that the concomitant administration of LP-Cur markedly restored the SiO_2-NPs mediated histopathological changes in the renal tissue indicating the nephroprotective property of LP-Cur against SiO_2-NPs toxicity. This finding was in accordance with El-Desoky *et al*. (2022); Machado *et al*. (2022) and Salimi *et al*. (2022) studies. The nephroprotective efficiency role of the LP-Cur might be attributed to its potent action inscavenging of ROS (Jurenka, 2009; Yu *et al*., 2011).

This study demonstrated that the renal tissue of SiO_2-NPs exposed rats (GpII) showed a substantial increase in the immunoreactivity of caspase-3 as compared to the control group (GpI). This result agreed with Mahmoud *et al*. (2019) and Azouz and Korany (2021) findings. Caspase-3 is one of the vital components in renal apoptosis (Jeruc *et al*., 2006; Ahmed *et al*., 2021). Initiation of caspase-3 can be mediated by intrinsic factors inducing mitochondrial damage and it plays a great role in cell apoptosis (Kusaczuk *et al*., 2018). Activation of caspase-3 is a great hallmark of DNA fragmentation and nuclear condensation in apoptotic cells (Albasher *et al*., 2020; Hashim *et al*., 2021). The renal cell death mediated by SiO_2-NPs could be attributed to excessive generation of ROS which lead to mitochondrial damage (Kusaczuk *et al*., 2018).

Oncountry, the renal tubular epitheliumof SiO_2-NPs exposed rats co-treated with LP-Cur showed a pronounced reduction in caspase-3 immunoreaction reflecting the anti-apoptotic action of LP-Cur. In this respect, Awad and El-Sharif (2011) illustrated that curcumin reduced apoptosis induction in renal tissue by inhibiting transforming growth factor-beta (TGF-β) and caspase-3. Numerous studies have demonstrated the potential protective effect of LP-Cur against oxidative stress and cell death (Liu *et al*., 2022; Noor *et al*., 2022; Salimi *et al*., 2022) which might be related to LP-Cur's ability to strengthen antioxidant defence systems and efficiently quench ROS (Jurenka, 2009; Yu *et al*., 2011; Dai *et al*., 2016). LP-Cur is efficient at scavenging ROS from cells, maintaining the levels of antioxidant enzymes, preventing damage to mitochondria and arresting the intrinsic apoptotic pathway (Choudhury *et al*., 2016).

Conclusion

The wide spread application of SiO_2-NPs owingto their physicochemical properties results in the increased possibilities of human exposure which make a great public health concern regarding their potential toxicity.This toxicity was observed through asignificant increase in BUN, creatinine, and MDA levels in addition to a decrease in GSH concentration. Furthermore, the SiO_2-NPs exposed group showed a pronounced alteration and distortionof renal tissue in addition to, a strong positive immu-

noreaction to caspase-3. These results demonstrate that the main risk factor in SiO_2-NPs-induced renal toxicity is oxidative stress. Interestingly, oral administration of LP-Cur (80 mg/kg/day) can significantly improve renal function parameters and reduce oxidative damage, histopathological changes and apoptosis caused by SiO_2-NPs intoxication (200 mg/kg/IP daily) for 30 days.According to these findings, LP-Cur improve the antioxidant capacity in addition to, its antiapoptotic action. Collectively, this research confirmed that LP-Cur had a strong protective effect against SiO_2-NPs induced renal toxicity.

Conflict of interest

The authors declare that they have no conflict of interest.

References

Abdelhalim, M.A.K., Jarrar, B.M., 2011. The appearance of renal cells cytoplasmic degeneration and nuclear destruction might be an indication of GNPs toxicity. Lipids Health Dis. 10, 1-6.

Ahmed, Y.H., El-Naggar, M.E., Rashad, M.M., Youssef, A., Galal, M.K., Bashir, D.W., 2022. Screening for polystyrene nanoparticle toxicity on kidneys of adult male albino rats using histopathological, biochemical, and molecular examination results. Cell Tissue Res. 388, 149-165.

Ahmed, Z.S.O., Galal, M.K., Drweesh, E.A., Abou-El-Sherbini, K.S., Elzahany, E.A., Elnagar, M.M., Yasin, N.A., 2021. Protective effect of starch-stabilized selenium nanoparticles against melamine-induced hepato-renal toxicity in male albino rats. Inter. J. Biol. Macromol. 191, 792-802.

Aillon, K.L., Xie, Y., El-Gendy, N., Berkland, C.J., Forrest, M.L. 2009. Effects of nanomaterial physicochemical properties on in vivo toxicity. Adv. Drug Deliv. Rev. 61, 457-466.

Albasher, G., Al Kahtani, S., Alwahibi, M.S., Almeer, R., 2020. Effect of Moringa oleifera Lam. methanolic extract on lead-induced oxidative stress-mediated hepatic damage and inflammation in rats. Environ. Sci. Pollut. Res. 27, 19877-19887.

Alhusaini, A., Fadda, L., Hassan, I., Ali, H.M., Alsaadan, N., Aldowsari, N., Alharbi, B., 2018. Liposomal curcumin attenuates the incidence of oxidative stress, inflammation, and DNA damage induced by copper sulfate in rat liver. Dose-Response 16, 3.

Almanaa, T.N., Aref, M., Kakakhel, M.A., Elshopakey, G.E., Mahboub, H.H., Abdelazim, A.M., Daoush, W.M., 2022. Silica nanoparticle acute toxicity on male rattus norvegicus domestica: ethological behavior, hematological disorders, biochemical analyses, hepato-renal function, and antioxidant-immune response. Front. Bioengin. Biotechnol. 10, 868111.

Almansour, M., Alarifi, S., Jarrar, B., 2018. In vivo investigation on the chronic hepatotoxicity induced by intraperitoneal administration of 10-nm silicon dioxide nanoparticles. Inter. J. Nanomed. 12, 2685-2696.

Almeida, J.P.M., Chen, A.L., Foster, A., Drezek, R., 2011. In vivo biodistribution of nanoparticles. Nanomedicine 6, 815-835.

Awad, A.S., El-Sharif, A.A., 2011. Curcumin immune-mediated and anti-apoptotic mechanisms protect against renal ischemia/reperfusion and distant organ induced injuries. Inter. Immunopharmacol. 11, 992-996.

Azouz, R.A., Korany, R.M., 2021. Toxic impacts of amorphous silica nanoparticles on liver and kidney of male adult rats: an in vivo study. Biol. Trace Elem. Res. 199, 2653-2662.

Badawy, M.M., Sayed-Ahmed, M.Z., Almoshari, Y., Alqahtani, S.S., Alshahrani, S., Mabrouk, H.A.A., Ahmed, D.A.M., 2023. Magnesium Supplementation Alleviates the Toxic Effects of Silica Nanoparticles on the Kidneys, Liver, and Adrenal Glands in Rats. Toxics 11, 381.

Bangham, A.D., 1993. Liposomes: the Babraham connection. Chem. Phys. Lipids 64, 275-285.

Bancroft, J.D., Gamble, M., 2008. Theory and practice of histological techniques. 6th edn, Churchill Livingston Edinburgh, London.

Birben, E., Sahiner, U.M., Sackesen, C., Erzurum, S., Kalayci, O., 2012. Oxidative stress and antioxidant defense. World Allergy Org. J. 5, 9-19.

Bogni, S., Ortner, M.A., Vajtai, I., Jost, C., Reinert, M., Dallemagne, B., Frenz, M., 2012. New laser soldering-based closures: a promising method in natural orifice transluminal endoscopic surgery. Gastrointest. Endoscop 76, 151-158.

Chan, W.T., Liu, C.C., Chiang Chiau, J.S., Tsai, S.T., Liang, C.K., Cheng, M.L., Hou, S.Y., 2017. In vivo toxicologic study of larger silica nanoparticles in mice. Inter. J. Nanomed. 12, 3421-3432.

Choudhury, S.T., Das, N., Ghosh, S., Ghosh, D., Chakraborty, S., Ali, N., 2016. Vesicular (liposomal and nanoparticulated) delivery of curcumin: a comparative study on carbon tetrachloride–mediated oxidative hepatocellular damage in rat model. Inter. J. Nanomed. 14, 2179-2193.

Dai, C., Li, D., Gong, L., Xiao, X., Tang, S., 2016. Curcumin ameliorates furazolidone-induced DNA damage and apoptosis in human hepatocyte L02 cells by inhibiting ROS production and mitochondrial pathway. Molecules 21, 1061.

El-Desoky, G.E., Wabaidur, S.M., AlOthman, Z.A., Habila, M.A., 2022. Evaluation of Nano-curcumin effects against Tartrazine-induced abnormalities in liver and kidney histology and other biochemical parameters. Food Sci. Nutr. 10, 1344-1356.

El Gamal, A.A., AlSaid, M.S., Raish, M., Al-Sohaibani, M., Al-Massarani, S.M., Ahmad, A., Rafatullah, S., 2014. Beetroot (Beta vulgaris L.) extract ameliorates gentamicin-induced nephrotoxicity associated oxidative stress, inflammation, and apoptosis in rodent model. Med. Inflam. 2014.

Ellman, G.L., 1959. Tissue sulfhydryl groups. Arch. Biochem. Biophys. 82, 70-77.

Florek, E., Witkowska, M., Szukalska, M., Richter, M., Trzeciak, T., Miechowicz, I., Giersig, M., 2023. Oxidative Stress in Long-Term Exposure to Multi-Walled Carbon Nanotubes in Male Rats. Antioxidants 12, 464.

Fritsch-Decker, S., Marquardt, C., Stoeger, T., Diabaté, S., Weiss, C., 2018. Revisiting the stress paradigm for silica nanoparticles: Decoupling of the anti-oxidative defense, pro-inflammatory response and cytotoxicity. Arch. Toxicol. 92, 2163-2174.

Fruijtier-Pölloth, C., 2012. The toxicological mode of action and the safety of synthetic amorphous silica—A nanostructured material. Toxicology 294, 61-79.

Gazia, M.A., El-Magd, M.A., 2019. Effect of pristine and functionalized multiwalled carbon nanotubes on rat renal cortex. Acta Histochemica 121, 207-217.

Gera, M., Sharma, N., Ghosh, M., Lee, S.J., Min, T., Kwon, T., Jeong, D.K., 2017. Nanoformulations of curcumin: An emerging paradigm for improved remedial application. Oncotarget 8, 66680.

Ghalandarlaki, N., Alizadeh, A.M., Ashkani-Esfahani, S., 2014. Nanotechnology-applied curcumin for different diseases therapy. BioMed Res. Inter. 2014, 394264.

Guo, M., Xu, X., Yan, X., Wang, S., Gao, S., Zhu, S., 2013. In vivo biodistribution and synergistic toxicity of silica nanoparticles and cadmium chloride in mice. J. Hazard. Mater. 260, 780-788.

Hamano, N., Böttger, R., Lee, S.E., Yang, Y., Kulkarni, J.A., Ip, S., Li, S.D. 2019. Robust microfluidic technology and new lipid composition for fabrication of curcumin-loaded liposomes: effect on the anticancer activity and safety of cisplatin. Mol. Pharmac. 16, 3957-3967.

Hashim, A.R., Bashir, D.W., Yasin, N.A., Galal, M.K., 2021. Ameliorative effect of N-acetylcysteine against glyphosate-induced hepatotoxicity in adult male albino rats: histopathological, biochemical, and molecular studies. Environ. Sci. Pollut. Res. 28, 42275-42289.

Hassankhani, R., Esmaeillou, M., Tehrani, A.A., Nasirzadeh, K., Khadir, F., Maadi, H., 2015. In vivo toxicity of orally administrated silicon dioxide nanoparticles in healthy adult mice. Environ. Sci. Pollut. Res. 22, 1127-1132.

Hewlings, S.J., Kalman, D.S., 2017. Curcumin: A review of its effects on human health. Foods 6, 92.

Hozayen, W.G., Mahmoud, A.M., Desouky, E.M., El-Nahass, E.S., Soliman, H.A., Farghali, A.A., 2019. Cardiac and pulmonary toxicity of mesoporous silica nanoparticles is associated with excessive ROS production and redox imbalance in Wistar rats. Biomed. Pharmacother. 109, 2527-2538.

Hsu, S. M., Raine, L., Fanger, H., 1981. The use of antiavidin antibody and avidin-biotin-peroxidase complex in immunoperoxidase technics. Amer. J. Clin. Pathol. 75, 816-821.

Jeruc, J., Vizjak, A., Rozman, B., Ferluga, D., 2006. Immunohistochemical expression of activated caspase-3 as a marker of apoptosis in glomeruli of human lupus nephritis. Amer. J. Kidney Dis. 48, 410-418.

Johar, D., Roth, J.C., Bay, G.H., Walker, J.N., Kroczak, T.J., Los, M., 2004. Inflammatory response, reactive oxygen species, programmed (necrotic-like and apoptotic) cell death and cancer. RocznikiAkademiiMedycznej w Bialymstoku 49, 31-39.

Joshi, S., Bawage, S., Tiwari, P., Kirby, D., Perrie, Y., Dennis, V., Singh, S.R., 2019. Liposomes: a promising carrier for respiratory syncytial virus therapeutics. Expert Opinion Drug Deliv. 16, 969-980.

Jurenka, J.S., 2009. Anti-inflammatory properties of curcumin, a major constituent of Curcuma longa: a review of preclinical and clinical research. Altern. Med. Rev. 14, 2.

Kim, J.H., Kim, C.S., Ignacio, R.M.C., Kim, D.H., Sajo, M.E.J., Maeng, E.H., Kim, S.K., 2014. Immunotoxicity of silicon dioxide nanoparticles with different sizes and electrostatic charge. Inter. J. Nanomed. 9, 183-193.

Kim, J.S., Kim, J.M., Son, J.A., Han, S.Y., Kim, C.T., Lee, N.S., Jeong, Y.G., 2008. Decreased calbindin-immunoreactive Renshaw cells (RCs) in the lumbar spinal cord of the ataxic pogo mice. Korean Journal of Anatomy 41, 255-263.

Kusaczuk, M., Krętowski, R., Naumowicz, M., Stypułkowska, A., Cechowska-Pasko, M., 2018. Silica nanoparticle-induced oxidative stress and mitochondrial damage is followed by activation of intrinsic apoptosis pathway in glioblastoma cells. Inter. J. Nanomed. 2279-2294.

Lee, J.A., Kim, M.K., Paek, H.J., Kim, Y.R., Kim, M.K., Lee, J.K., Choi, S.J., 2014. Tissue distribution and excretion kinetics of orally administered silica nanoparticles in rats. Inter. J. Nanomed. 9, 251-260.

Liang, C.L., Xiang, Q., Cui, W.M., Jin, F.A., Sun, N.N., Zhang, X.P., Jia, X.D., 2018. Subchronic oral toxicity of silica nanoparticles and silica microparticles in rats. Biomed. Environ. Sci. 31, 197-207.

Liu, Z., Shi, B., Wang, Y., Xu, Q., Gao, H., Ma, J., Yu, W., 2022. Curcumin alleviates aristolochic acid nephropathy based on SIRT1/Nrf2/HO-1 signaling pathway. Toxicology 479, 153297.

Machado, D.I., de Oliveira Silva, E., Ventura, S., Vattimo, M.D., 2022. The effect of curcumin on renal ischemia/reperfusion injury in diabetic rats. Nutrients 14, 2798.

Mahmoud, A.M., Desouky, E.M., Hozayen, W.G., Bin-Jumah, M., El-Nahass, E.S., Soliman, H.A., Farghali, A.A. 2019. Mesoporous silica nanoparticles trigger liver and kidney injury and fibrosis via altering TLR4/NF-κB, JAK2/STAT3 and Nrf2/HO-1 signaling in rats. Biomolecules 9, 528.

Manconi, M., Isola, R., Falchi, A.M., Sinico, C., Fadda, A.M., 2007. Intracellular distribution of fluorescent probes delivered by vesicles of different lipidic composition. Colloids and Surfaces B: Biointerfaces 57, 143-151.

Mehdi, L.A., Al-Husseini, A.M., 2021. Estimate toxic effect of silica nanoparticles on kidney, liver and lung function of male albino rats. Syst. Rev. Pharm. 12, 570-575.

Mohamed, N.A., Saleh, S.M., 2010. Effect of Pre and Postnatal Exposure to Lead Acetate on the Kidney of Male Albino Rat: A Light and Electron Microscopic Study. Egypt J. Histol. 33, 365–379.

Murugadoss, S., Lison, D., Godderis, L., Van Den Brule, S., Mast, J., Brassinne, F., Hoet, P.H., 2017. Toxicology of silica nanoparticles: an update. Arch. Toxicol. 91, 2967-3010.

Nabeshi, H., Yoshikawa, T., Matsuyama, K., Nakazato, Y., Arimori, A., Isobe, M., Tsutsumi, Y., 2012. Amorphous nanosilicas induce consumptive coagulopathy after systemic exposure. Nanotechnology 23, 045101.

Nalli, M., Ortar, G., Moriello, A.S., Di Marzo, V., De Petrocellis, L., 2017. Effects of curcumin and curcumin analogues on TRP channels. Fitoterapia 122, 126-131.

Nemmar, A., Yuvaraju, P., Beegam, S., Yasin, J., Kazzam, E.E., Ali, B.H., 2016. Oxidative stress, inflammation, and DNA damage in multiple organs of mice acutely exposed to amorphous silica nanoparticles. Inter. J. Nanomed. 919-928.

Noor, N.A., Hosny, E.N., Khadrawy, Y.A., Mourad, I.M., Othman, A.I., Aboul Ezz, H.S., Mohammed, H.S., 2022. Effect of curcumin nanoparticles on streptozotocin-induced male Wistar rat model of Alzheimer's disease. Metabolic Brain Dis. 37, 343-357.

Ohkawa, H., Ohishi, N., Yagi, K., 1979. Assay for lipid peroxides in animal tissues by thiobarbituric acid reaction. Analyt. Biochem. 95, 351-358.

Puca, A., Albanese, A., Esposito, G., Maira, G., Tirpakova, B., Rossi, G., Pini, R., 2006. Diode laser-assisted carotid bypass surgery: an experimental study with morphological and immunohistochemical evaluations. Neurosurgery 59, 1286-1295.

Rai, B., Kaur, J., Catalina, M., 2010. Anti–oxidation actions of curcumin in two forms of bed rest: oxidative stress serum and salivary markers. Asian Pac. J. Trop. Medicine 3, 651-654.

Salimi, A., Kheiripour, N., Jouzdani, A.F., Ghasemi, H., Asl, S.S., Ghafouri-Khosrowshahi, A., Ranjbar, A., 2022. Nanocurcumin Improves Lipid Status, Oxidative Stress, and Function of the Liver in Aluminium Phosphide-Induced Toxicity: Cellular and Molecular Mechanisms. BioMed Res. Inter. 2022.

Schrand, A.M., Rahman, M.F., Hussain, S.M., Schlager, J.J., Smith, D.A., Syed, A.F., 2010. Metal-based nanoparticles and their toxicity assessment. Wiley interdisciplinary Rev.: Nanomed. Nanobiotechnol. 2, 544-568.

Shehzad, A., Qureshi, M., Anwar, M.N., Lee, Y.S., 2017. Multifunctional curcumin mediate multitherapeutic effects. J. Food Sci. 82, 2006-2015.

Signorell, R.D., Luciani, P., Brambilla, D., Leroux, J.C., 2018. Pharmacokinetics of lipid-drug conjugates loaded into liposomes. Europ. J. Pharmac. Biopharmac. 128, 188-199.

Storka, A., Vcelar, B., Klickovic, U., Gouya, G., Weisshaar, S., Aschauer, S., Wolzt, M., 2013. Effect of liposomal curcumin on red blood cells in vitro. Anticancer Res. 33, 3629-3634.

Sun, A., Qian, D., Wang, Z., Xu, Y., Ye, H., Fang, C.J., Yan, C.H., 2021. Protective effect of lipoic acid modification on brain dysfunctions of mice induced by mesoporous silica nanoparticles. Che Engin. J. 415, 128957.

Sun, L., Li, Y., Liu, X., Jin, M., Zhang, L., Du, Z., Sun, Z., 2011. Cytotoxicity and mitochondrial damage caused by silica nanoparticles. Toxicology in vitro 25, 1619-1629.

Vance, M.E., Kuiken, T., Vejerano, E.P., McGinnis, S.P., Hochella Jr, M.F., Rejeski, D., Hull, M.S., 2015. Nanotechnology in the real world: Redeveloping the nanomaterial consumer products inventory. Beilstein J. Nanotechnol. 6, 1769-1780.

Wang, H., Wang, J., Deng, X., Sun, H., Shi, Z., Gu, Z., Liu, Y., Zhao, Y., 2004. Biodistribution of carbon single-wall carbon nanotubes in mice. J. Nan. Nanotechnol. 4, 1019-1024.

Wei, X.Q., Zhu, J.F., Wang, X.B., Ba, K., 2020. Improving the stability of liposomal curcumin by adjusting the inner aqueous chamber pH of liposomes. ACS omega 5, 1120-1126.

WHO (World Health Organization), 2017. WHO guidelines on protecting workers from potential risks of manufactured nanomaterials. https://www.who.int/publications-detail-redirect/9789241550048

Wu, L., Jiang, C., Kang, Y., Dai, Y., Fang, W., Huang, P., 2020. Curcumin exerts protective effects against hypoxia reoxygenation injury via the enhancement of apurinic/apyrimidinic endonuclease 1 in SH SY5Y cells: involvement of the PI3K/AKT pathway. Inter. J. Mol. Med. 45, 993-1004.

Xia, T., Kovochich, M., Brant, J., Hotze, M., Sempf, J., Oberley, T., Nel, A.E 2006. Comparison of the abilities of ambient and manufactured nanoparticles to induce cellular toxicity according to an oxidative stress paradigm. Nano letters 6, 1794-1807.

Yazdimamaghani, M., Moos, P.J., Ghandehari, H., 2018. Global gene expression analysis of macrophage response induced by nonporous and porous silica nanoparticles. Nanomed.: Nanotechnol., Biol. Med. 14, 533-545.

Yu, H., Li, J., Shi, K., Huang, Q., 2011. Structure of modified ε-polylysine micelles and their application in improving cellular antioxidant activity of curcuminoids. Food & function 2, 373-380.

Zheng, Q.T., Yang, Z. H., Yu, L. Y., Ren, Y.Y., Huang, Q. X., Liu, Q., Zheng, X., 2017. Synthesis and antioxidant activity of curcumin analogs. J. Asian Natural Products Res. 19, 489-503.